Sensors & Actuators: B. Chemical 445 (2025) 138626

Contents lists available at ScienceDirect

Sensors and Actuators: B. Chemical

journal homepage: www.elsevier.com/locate/snb

Fluorogenic legumain-activated aiegen probe enables real-time *in Vivo* diagnosis of schistosomiasis mansoni

Qiang Li [a], Chenxu Yan [b], Jing Xu [a], Chunli Cao [a], Liping Duan [a], Yinlong Li [a], Wangping Deng [a], Zhiqiang Qin [a], Qingchi Han [a], Yingjun Qian [a], Nicholas Midzi [c], Masceline Jenipher Mutsaka-Makuvaza [c,d], Xiaonong Zhou [a], Shizhu Li [a,*], Zhiqian Guo [b,*]

[a] *National Key Laboratory of Intelligent Tracking and Forecasting for Infectious Diseases, National Institute of Parasitic Diseases at Chinese Center for Disease Control and Prevention, Chinese Center for Tropical Diseases Research, National Research Center for Tropical Diseases, Key Laboratory of Parasite and Vector Biology, National Health Commission, WHO Collaborating Center for Tropical Diseases, National Center for International Research on Tropical Diseases, Ministry of Science and Technology, Shanghai 20025, China*

[b] *Key Laboratory for Advanced Materials and Joint International Research Laboratory of Precision Chemistry and Molecular Engineering, Institute of Fine Chemicals, Frontiers Science Center for Materiobiology and Dynamic Chemistry, School of Chemistry and Molecular Engineering, East China University of Science and Technology, Shanghai 200237, China*

[c] *National Institute of Health Research, Ministry of Health and Child Care, P.O. Box CY573, Causeway, Harare, Zimbabwe*

[d] *Department of Microbiology and Parasitology, College of Medicine and Health Sciences, University of Rwanda, Butare, Rwanda*

ARTICLE INFO

Keywords:
Fluorescent probe
AIEgen
Legumain
Schistosomiasis Mansoni

ABSTRACT

Legumain is increasingly recognized as a biomarker for schistosomiasis because of its crucial involvement in cellular biochemistry and pathogenesis. However, its precise biological roles remain insufficiently understood. To characterize the biological significance of legumain activity in schistosomiasis mansoni progression, we developed a legumain-activatable, aggregation-induced emission (AIE) near-infrared (NIR) fluorescent probe, QM-AAN-CPP. This probe incorporates Quinoline-Malononitrile (QM) as the fluorescence reporter, an alanine-alanine-asparagine (AAN) peptide sequence as the specific substrate for legumain, and a cell-penetrating peptide (CPP) moiety for enhanced targeting and solubility. *In vitro*, QM-AAN-CPP exhibited excellent sensitivity, high selectivity, and robust stability, facilitating accurate detection of legumain activity in living adult *Schistosoma mansoni* worms through fluorescence imaging. *In vivo* fluorescence imaging further demonstrated that QM-AAN-CPP detected legumain activity predominantly in the intestinal region of infected subjects, highlighting the probe's potential for real-time disease monitoring. Overall, this enzyme-activatable AIE&NIR probe, QM-AAN-CPP, shows promise as a tool for elucidating legumain's role in the pathogenesis of schistosomiasis mansoni and offers new avenues for advanced diagnostic strategies.

1. Introduction

Schistosomiasis is a parasitic disease caused by flukes of the genus *Schistosoma* that remains widespread in tropical and subtropical regions, primarily affecting communities lacking adequate sanitation [1,2]. Currently, approximately 250 million people are infected with schistosomiasis, and the World Health Organization (WHO) classifies it as a Neglected Tropical Disease (NTD). In terms of socioeconomic burden and public health impact, schistosomiasis ranks second only to malaria [3,4]. Despite its high prevalence, existing diagnostic methods still face notable limitations [5–8]. Although the Kato-Katz technique, a microscopy-based detection technology, is considered the gold standard for detecting schistosomiasis, its sensitivity is relatively low [9]. While polymerase chain reaction (PCR) methods can be more sensitive, they are labor-intensive and not easily portable [10]. Many other traditional diagnostic approaches encounter similar drawbacks. Consequently, new diagnostic approaches and biomarkers are urgently needed to achieve high sensitivity, specificity, and portability. In this regard, fluorescent probes present several advantages over traditional methods, including high selectivity, excellent sensitivity, rapid response, and a non-invasive workflow. These properties make them particularly useful for real-time tracking, visualization of dynamic changes in live samples, and specific

* Corresponding authors.
E-mail addresses: lisz@chinacdc.cn (S. Li), guozq@ecust.edu.cn (Z. Guo).

https://doi.org/10.1016/j.snb.2025.138626
Received 7 May 2025; Received in revised form 9 August 2025; Accepted 28 August 2025
Available online 29 August 2025

species detection [11–13].

Legumain [14–16], a cysteine proteinase first discovered in legumes and subsequently in parasites (*Schistosoma mansoni*, nematodes) and mammals, is suggested to have multiple intra- and extracellular functions. According to the literature [17–19], legumain was an stable endogenous lysosomal protease and considered as a reliable potential biomarker of schistosomiasis detection. And leguamin was expressed at high levels in the gut after invasion of the vertebrate host by infectious forms called cercariae. Given its importance in *Schistosoma mansoni* biology, legumain is gaining increasing attention as a potential biomarker for the diagnosis of schistosomiasis. Therefore, *in vivo* imaging of legumain activity may facilitate the early detection of schistosomiasis and allow for the assessment of therapeutic interventions. In the past few years, several studies have developed different probes to image legumain in vivo, mainly in terms of tumors [20,21].

Aggregation-induced emission (AIE) [22,23] is a powerful approach for identifying protein biomarkers, particularly due to its characteristic light-up response in binding events during aggregation. In the context of *in vivo* imaging, near-infrared (NIR) fluorescence offers deeper tissue penetration and reduced autofluorescence, making it highly advantageous for non-invasive diagnostics [24,25]. Quinoline-Malononitrile (QM) is a widely utilized AIE organic dye with excellent optical properties and can be readily modified to achieve emission in the NIR region. QM has been extensively studied as the core component in various QM-based probes, enabling activatable bioimaging and therapeutic applications [26,27].

In this study, we developed a schistosome-targeted AIE probe (QM-AAN-CPP) for *in vivo* imaging of legumain in schistosomiasis. QM-AAN-CPP (Scheme 1) comprises three components: (i) a QM unit for activatable fluorescence; (ii) an alanine-alanine-asparagine (AAN) peptide sequence that specifically recognizes and is cleaved by legumain [28,29]; and (iii) a hydrophilic biocompatible cell-penetrating peptide (CPP) [30,31] that confers water solubility, maintains the probe in a fluorescence-off state under physiological conditions, and facilitates tissue penetration. Moreover, the positively charged CPP aids in targeting the surface of adult *Schistosoma mansoni* worms [32,33]. We confirmed that the probe maintains an initial fluorescence-off state, owing to the excellent water solubility conferred by the CPP. Notably, when QM-AAN-CPP encounters legumain, the AAN unit is cleaved, releasing QM and triggering a robust AIE&NIR light-up response. This mechanism enables sensitive and specific detection of legumain activity.

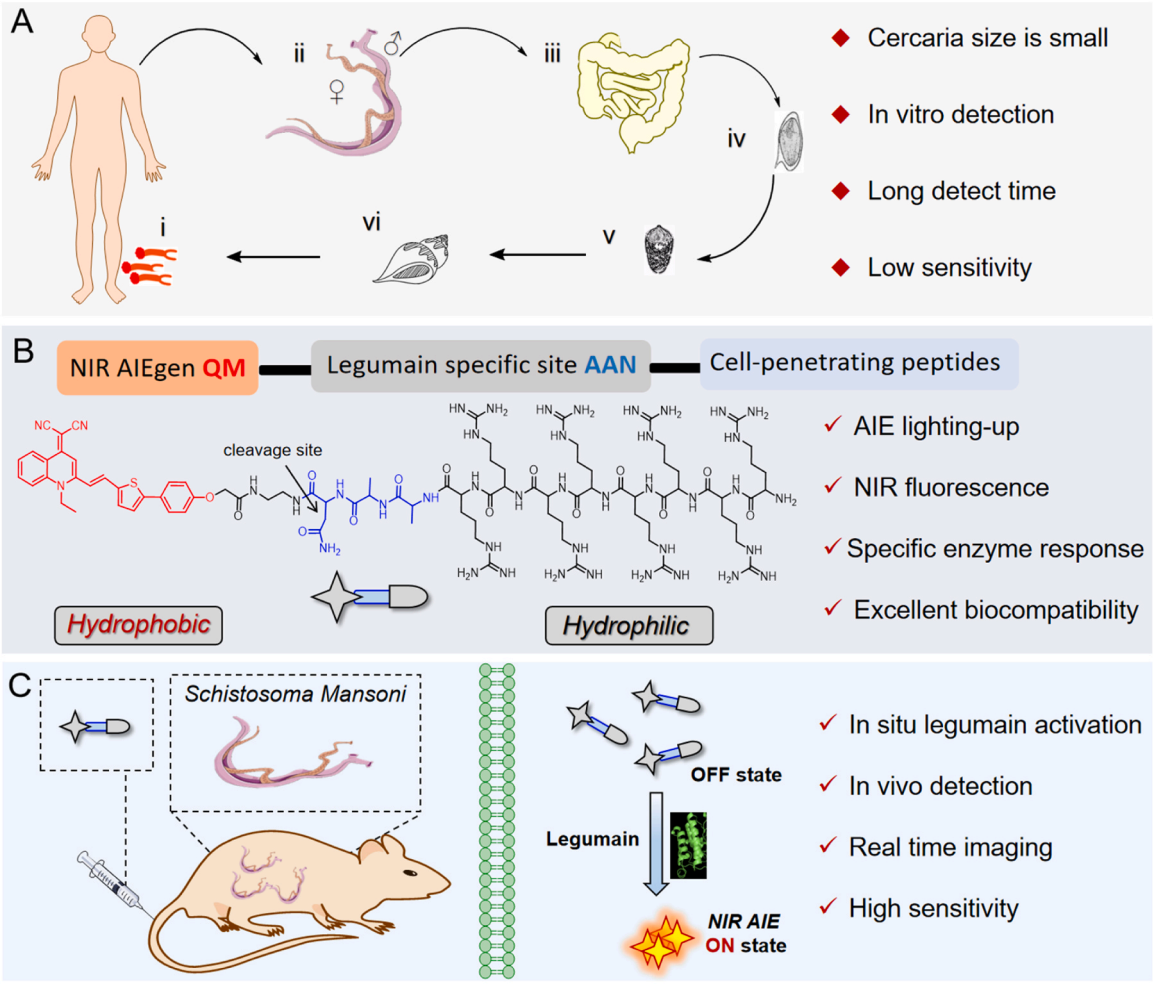

Scheme 1. Legumain specific, activatable AIE fluorescent platform QM-AAN-CPP for schistosomiasis diagnosis and real-time tracking. (A) Showing the relationship between the life cycle of schistosomes: i) cercariae penetrate shin; ii) cercariae lose tail and become schistosomulae, then schistosomulae mature into adult worms; iii) parired adult schistosomes migrate to the bowel, rectum et al.; iv) adult schistosomes released the eggs and eggs shed into faeces; v) eggs hatch into miracidia in freshwater; vi) miracidia infect snail, and miracidia undergoes asexual reproduction to form sporocyst, then snail releases the free-swimming cercaria, creating a cycle of infection. (B) Structure of the QM-AAN-CPP probe and design principle. The probe comprises: i) a fluorophore QM (AIE component); ii) an AAN substrate as the recognition unit cleaved by legumain; iii) a positively charged CPP which enhances biocompatibility, and targeting of the *Schistosoma mansoni* surface. (C) Upon accumulation in *Schistosoma mansoni*, QM-AAN-CPP is activated by legumain, producing an AIE&NIR fluorescence signal for effective imaging.

2. Experimental section

2.1. Synthesis and characterization

Detailed information regarding reagents and instruments used in this study can be found in the Supplementary Material. The synthesis route is illustrated in Scheme S1.

Synthesis of 4-(5-formylthiophen-2-yl)phenol (**compound 3)**. 4-hydroxyphenylboronic acid (240 mg, 1.73 mmol), 5-bromothiophene-2-carboxaldehyde (380 mg, 2.0 mmol) and Tetrakis(triphenylphosphine)palladium (120 mg, 0.1 mmol) were dissolved in tetrahydrofuran (24 mL) and K_2CO_3 aqueous solution (2 mol/L, 12 mL) under argon protection. The mixture was refluxed for 8 h. After the reaction system was cooled to room temperature, added 30 mL water, and then extract it three times with 30 mL dichloromethane, and dry with anhydrous sodium sulfate. The solvent was then removed by rotary evaporation, and the crude product was purified by silica gel chromatography (DCM/EA=15:1, v/v) to afford the pure product 3 (195 mg) as a yellow solid, yield (59 %). ^{1}H NMR (400 MHz, DMSO-d_6, ppm) : δ 10.03 (s, 1 H, -OH), 9.85 (s, 1 H, -CHO), 7.99 (d, J = 4.0 Hz, 1 H, thiophene-H), 7.65 (d, J = 8.7 Hz, 2 H, phenyl-H), 7.57 (d, J = 4.0 Hz, 1 H, thiophene-H), 6.87 (d, J = 8.7 Hz, 2 H, phenyl-H). ^{13}C NMR (100 MHz, DMSO-d_6, ppm): δ 116.10, 123.47, 127.86, 139.54, 140.40, 153.69, 158.97, 183.61. Mass spectrometry (ESI-MS, m/z): [M-H]$^-$ calcd. for $C_{11}H_8O_2S$: 203.0161; found: 203.0167.

Synthesis of **QM-S-OH**. QM (399 mg, 1.69 mmol) and compound 3 (230 mg, 1.13 mmol) were dissolved in acetonitrile (25 mL) with piperidine (1 mL) under argon protection. The mixture was refluxed for 8 h. After the reaction system was cooled to room temperature, a large amount of orange-red solids were separated out. The solvent was then removed by filtration, and the crude product was purified by silica gel chromatography (DCM/MeOH=10:1, v/v) to afford the pure product QM-S-OH (286 mg) as an orange-yellow solid, yield (60 %). ^{1}H NMR (400 MHz, DMSO-d_6, ppm) : δ 8.93 (q, J =8.5 Hz, 1 H, phenyl-H), 8.09 (d, J = 9.0 Hz, 1 H, phenyl-H), 7.94 (t, J = 11.6 Hz, 1 H, phenyl-H), 7.68 (d, J = 14.4 Hz, 1 H, thiophene-H), 7.62 (t, J = 7.2 Hz, 1 H, phenyl-H), 7.55 (t, J=5.2 Hz, 3 H, phenyl-H), 7.40 (d, J = 3.6 Hz, 1 H, phenyl-H),7.13 (d, J = 15.5 Hz, 1 H, thiophene-H), 7.03 (s, 1 H, quinoline-H), 6.84 (d, J = 8.6 Hz, 2 H, alkene-H), 4.56 (q, J = 7.1 Hz, 2 H, -CH_2CH$_3$), 1.43 (t, J = 7.1 Hz, 3 H, -CH$_3$). ^{13}C NMR (100 MHz, DMSO-d_6, ppm): δ 13.61, 43.79, 46.43 106.28, 106.35, 116.67, 116.95, 118.02, 119.38, 120.55, 121.77, 122.03, 125.06, 127.05, 133.09, 133.62, 136.82, 137.88, 148.02, 148.64, 151.88. Mass spectrometry (ESI-MS, m/z): [M+H]$^+$ calcd. for $C_{26}H_{19}N_3OS$: 422.1327; found: 422.1319.

Synthesis of **QM-S-COOH**. Under an argon atmosphere, QM-S-OH (240 mg, 0.533 mmol), ethyl bromoacetate (112 mg, 0.66 mmol) and potassium carbonate (130 mg, 0.939 mmol) were dissolved under stirring in acetonitrile (15 mL). The mixture was then stirred refluxed for 12 h. The solvent was removed by filtration, and the crude product (150 mg) was then dissolved in THF (20 mL) with gradually adding 5 mL NaOH solution (90 mg, 2.25 mmol). The mixture was stirred at room temperature for 10 h. After adjusting pH to 5 with glacial acetic acid, the solvent was taken up in sat. NaCl, and extracted with CH_2Cl_2 (30 mL). Next, the solution was dried over anhydrous Na_2SO_4 and the solvent was removed under reduced pressure. Finally, the crude product was purified by silica gel chromatography with (DCM/PE=5:1, v/v) to afford the desired product QM-S-COOH (50 mg): yield 25 %. ^{1}H NMR (400 MHz, DMSO-d_6, ppm) : δ 8.93 (D, J =8.3 Hz, 1 H, phenyl-H), 8.07 (d, J = 8.4 Hz, 1 H, phenyl-H), 7.92 (d, J = 6.2 Hz, 1 H, phenyl-H), 7.64 (m, 5 H, one for thiophene-H, four for phenyl-H), 7.46 (s, 1 H, phenyl-H), 7.14 (d, J = 15.4 Hz, 2 H, thiophene-H), 6.99 (t, 3 H, two for alkene-H, four for phenyl-H), 4.65 (s, 2 H, - OCH_2COO -), 4.54 (d, J = 6.0 Hz, 2 H, -CH_2CH$_3$), 1.40 (s, 3 H, -CH$_3$). ^{13}C NMR (100 MHz, CD$_4$O, ppm): δ 22.49, 29.50, 47.40, 49.00, 68.19, 68.84, 106.83, 109.50, 112.67, 118.77, 118.89, 119.80, 121.04, 121.20, 122.31, 125.52, 126.97, 133.05, 133.33, 133.87, 137.57, 138.89, 148.08, 150.41, 150.75, 152.54, 171.90. Mass spectrometry (ESI-MS, m/z): [M+H]$^+$ calcd. for $C_{28}H_{22}N_3O_3S$: 480.1382; found: 480.1387.

Synthesis of **QM-AAN-CPP**. QM-AAN-CPP were synthesized by Shanghai Science Peptide Biological Technology Co., Ltd. ^{1}H NMR (400 MHz, CD$_4$O, ppm) : δ 8.97 (d, J =8.e Hz, 1 H, phenyl-H), 7.96 (d, J = 8.8 Hz, 1 H, phenyl-H), 7.87 (t, J = 8.4 Hz, 1 H, phenyl-H), 7.61 (d, J = 8.8 Hz, 2 H, phenyl-H), 7.52 (m, 2 H, one for thiophene-H, one for phenyl-H), 7.36 (d, J=3.6 Hz, 1 H, phenyl-H), 7.28 (d, J=3.6 Hz, 1 H, thiophene-H), 7.08 (s, 1 H, quinoline-H), 7.01 (m, 3 H, two for alkene-H, one for phenyl-H), 4.63 (t, J = 6.4 Hz, 1 H, Asn(N) -CO-CH(NH)-CH$_2$-), 4.54 (s, 2 H, -OCH_2-COO-), 4.52 (d, J = 7.2 Hz, 2 H, -CH_2CH$_3$), 4.54 (m, 7 H, Arg(R) -CO-CH(NH)-CH$_2$-), 4.23 (q, J = 10.0 Hz, 2 H, Ala(A) -CO-CH(CH$_3$)-NH-), 4.01 (t, J = 6.0 Hz, 1 H, Arg(R) -CO-CH(NH$_2$)-CH$_2$-), 3.45 (t, J = 4.4 Hz, 2 H, -NH-CH_2-CH$_2$-NH-), 3.39 (t, J = 5.2 Hz, 2 H, -NH-CH$_2$-CH_2-NH-), 3.20 (s, 16 H, Arg(R) -NH-CH_2-CH$_2$-CH$_2$-), 2.76 (d, J = 4.8 Hz, 2 H, Asn(N) -CO-CH(NH)-CH_2-), 1.90 (m, 16 H, Arg(R) -NH-CH$_2$-CH_2-CH$_2$-), 1.70 ((m, 16 H, Arg(R) -NH-CH$_2$-CH$_2$-CH_2-), 1.53 (t, J = 8.4 Hz, 3 H, -CH$_2$CH_3), 1.39 (t, J =7.2 Hz, 6 H, Ala(A) -CO-CH(CH_3)-NH-). ^{13}C NMR (100 MHz, CD$_4$O, ppm): δ 14.16, 17.28, 17.72, 25.17, 26.29, 29.93, 41.99, 54.97, 108.18, 116.51, 116.75, 118.65, 118.73, 119.66, 122.65, 124.67, 127.12, 128.26, 128.64, 133.47, 134.34, 134.82, 139.66, 140.14, 148.14, 149.98, 154.56, 158.72, 158.77, 159.35, 162.74, 163.09, 163.43, 171.36, 173.39, 174.01, 174.38, 174.45, 174.49, 175.02. Mass spectrometry (positive ion mode for [M + 3 H]/3$^+$): Calcd. for 676.68; found: 676.75. HPLC retention time: 13.786 min, Peak area: 95 %.

2.2. HPLC test of QM-AAN-CPP

The purity of the probe QM-AAN-CPP was detected by gradient elution. The analytial column type was Inertsil ODS-SP (4.6 mm*250 mm* 5um). The total flow rate was 1 mL/min, and the detect wavelength was 214 nm. The pump A: 0.1 %Trifluoroacetic in 100 % water, and the pump B: 0.1 %Trifluoroacetic in 100 % acetonitrile. The dissolution method was 15 % ACN+ 85 % H_2O, and the injected volume was 25 μL. The specific gradient elution time and dosage ratio can be found in the Table S1.

2.3. In vitro cytotoxicity assay

The human hepatocyte QSG-7701 cell line was purchased from the Institute of Cell Biology (Shanghai, China). The cell cytotoxicity of QM-AAN-CPP to QSG-7701 cells and were measured by 3-(4,5-dimethylthiazol-2-yl)-2,5-diphenyltetrazolium bromide (MTT) assay. The cytotoxicity was evaluated by Cell Counting Kit-8 (Dojindo, Tokyo, Japan) according to the factory's instruction. Cells were plated in 96-well plates in 0.1 mL volume of DMEM or RPMI-1640 medium with 10 % FBS, at a density of 1×10^4 cells/well and added with desired concentrations of QM-AAN-CPP. After incubation for 24 h, absorbance was measured with a Tecan GENios Pro multifunction reader (Tecan Group Ltd., Maennedorf, Switzerland). Each concentration was measured in triplicate and used in three independent experiments. The relative cell viability was calculated by the equation: cell viability (%) = ($OD_{treated}/OD_{control}$) × 100 %.

2.4. Schistosome mansoni imaging

The Schistosome mansoni cercaria were from National Institute of Health Research, Ministry of Health and Child Care (Zimbabwe). Schistosome mansoni cercaria and *Schistosoma mansoni* were seeded onto glass-bottom Petri dishes in culture medium (1.5 mL) separately, and allowed to adhere for 4 h before imaging. Probe QM-AAN-CPP at a final concentration of 25 μM (containing 0.1 % DMSO) were added into culture medium and incubated for 2 h at 37 °C under a humidified 5 % CO_2 atmosphere. Subsequently, the Schistosome mansoni cercaria and *Schistosoma mansoni* were transferred to a confocal dish for incubation,

followed by washing with physiological saline and imaging.

2.5. Animal experiments

The experimental mice were Balb/C mouse, (12–15 g, female and 20–30 g, male) were provided by the Laboratory Animal Research Center of the National Institute of Parasitic Diseases at Chinese Center for Disease Control and Prevention, Chinese Center for Tropical Diseases Research, National Research Center for Tropical Diseases (Shanghai, China). Male mice were infected with Schistosomiasis mansoni cercaria and kept for 50 days. Female mice served as controls and were not infected.

3. Results and discussion

3.1. Design of the probe QM-AAN-CPP

As typical laser dyes, QM derivatives possess key advantages for fluorescence applications, including pronounced aggregation behavior, extended emission wavelengths, and tunable photophysical characteristics. According to the literature[34], QM-COOH exhibits classic AIE features (Figure S1) and has been utilized in the diagnosis of enzyme-activated diseases. Building on QM-COOH, we optimized its structure to produce QM-S-COOH (Figure S2), which preserves the AIE characteristics (Fig. 1A) while shifting the fluorescence emission peak from 580 nm to 625 nm (Figure S2). More importantly, QM-S-COOH shows a spectral tail in the NIR region above 650 nm. Next, we synthesized QM-AAN-CPP with AIE&NIR properties. To achieve legumain-responsive fluorescence, we incorporated AAN, a specific recognition motif for legumain detection in living organisms. To overcome the solubility constraints common to AIE probes, we included a hydrophilic biocompatible CPP. The CPP moiety not only enhances tissue penetration but also enables on-site monitoring of endogenous legumain in *Schistosoma mansoni* and in living animal models.

3.2. Spectroscopic characteristics of QM-AAN-CPP

After synthesizing and characterizing QM-AAN-CPP, we investigated its optical properties *in vitro*. As shown in Figure S3, QM-AAN-CPP had two absorption maxima at 400 nm and 455 nm. Upon addition of legumain, these absorption peaks remained unchanged, indicating that the intrinsic structure of the QM chromophore was not altered. Because of the excellent water solubility of the CPP, QM-AAN-CPP remained well-dispersed in this system and thus initially exhibited negligible fluorescent emission. However, in the presence of excess legumain, the AAN segment was recognized and cleaved, releasing the QM derivatives, which emitted a strong fluorescence peak at 625 nm (Figure S4). High-performance liquid chromatography (HPLC) further confirmed the specific cleavage mechanism of QM-AAN-CPP by studying the enzyme-sensing mechanism. As shown in Fig. 1D, intact QM-AAN-CPP showed a narrow peak at a retention time of 4.2 min, whereas QM-S-COOH exhibited a distinct peak at 6.6 min. Following incubation of QM-AAN-CPP with legumain for 1 h, the original peak at 4.2 min markedly decreased, and a new narrow peak at approximately 6.2 min was observed, corresponding to QM-S-COOH derivatives. The change in fluorescence emission and HPLC confirmed that QM-AAN-CPP was specifically recognized by legumain. We next optimized the concentration (Fig. 1B) and incubation time (Fig. 1C) for maximal fluorescence output. QM-AAN-CPP (25 μM) yielded the highest fluorescence intensity in the presence of 5 μg/mL legumain after 4 h of incubation. HPLC analyses also corroborated these concentrations (Fig. 1E) and times (Fig. 1F). To gain a better understanding of the substrate-enzyme interactions between QM-AAN-CPP and legumain, the Michaelis−Menten kinetics model was adopted. Our enzyme kinetics data showed that QM-AAN-CPP served as an excellent probe for legumain, explaining the rapid turn-on response (Figure S5). In addition, the FL intensity at

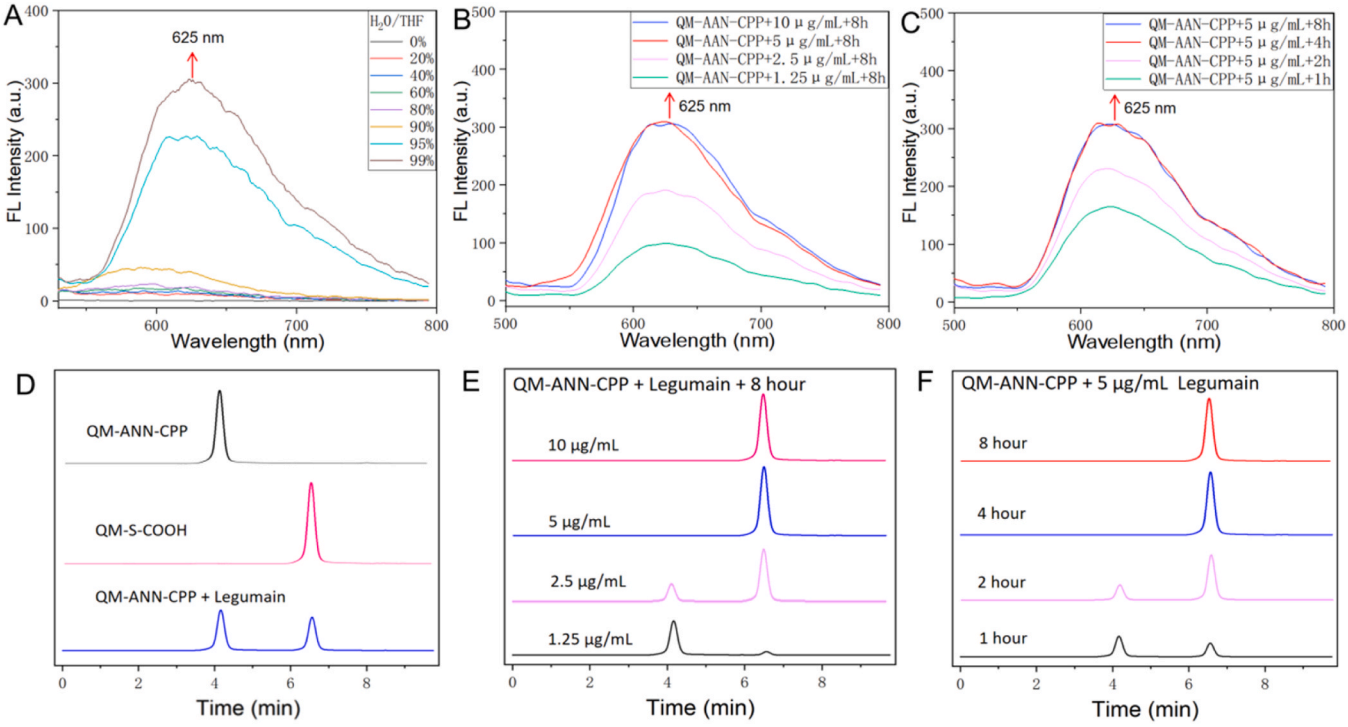

Fig. 1. (A) Fluorescence intensity of QM-S-COOH (10 μM) in a THF-water mixture (λ_{ex} = 455 nm). (B) Fluorescence intensity of QM-AAN-CPP (25 μM) incubated with legumain at 1.25, 2.5, 5 and 10 μg/mL for 8 h. (C) Fluorescence intensity of QM-AAN-CPP (25 μM) incubated with 5 μg/mL legumain for 1, 2, 4 and 8 h (λ_{ex} = 455 nm, λ_{em} = 550–780 nm). (D) Reverse-phase HPLC chromatogram of QM-AAN-CPP, QM-S-COOH, and QM-AAN-CPP incubated with legumain for 1 h. λ_{ex} = 455 nm. The retention times for QM-AAN-CPP and QM-S-COOH are 4.2 min and 6.6 min, respectively. (E) HPLC traces of QM-AAN-CPP (25 μM) incubated with legumain at 1.25, 2.5, 5 and 10 μg/mL for 8 h. (F) HPLC traces of QM-AAN-CPP (25 μM) incubated with 5 μg/mL legumain for 1, 2, 4 and 8 h.

625 nm of QM-AAN-CPP displayed a good linear relationship with the concentration of legumain in the range of 0–5 μg/mL (Figure S6), and the limit of detection (LOD) was determined to be 10.6 ng/mL for QM-AAN-CPP.

3.3. *In vitro stability and selectivity of QM-AAN-CPP*

The stability of AIE fluorophores is critical for practical applications [35], especially in the biological detection of legumain. Before applying QM-AAN-CPP in living organisms, we evaluated its stability by incubating the probe in fetal bovine serum (FBS) at 37°C. Fluorescence intensity and HPLC measurements were taken over multiple days. As shown in Fig. 2A, samples containing QM-AAN-CPP alone (without legumain) exhibited no detectable fluorescence over time. Conversely, when QM-AAN-CPP was incubated with legumain, strong fluorescence signals were observed across different days (Fig. 2B). HPLC analyses further confirmed that the probe remained stable under these conditions (Fig. 2C).

High selectivity under physiological conditions is equally important [36]. Therefore, we next investigated the fluorescence response of QM-AAN-CPP in the presence of various potential interfering species, including biological thiols (GSH, HCy, Cys), reactive oxygen species (ClO^-, H_2O_2), and common *Schistosoma* markers (LAP, Cathepsin B, legumain) [37–39]. As shown in Fig. 2D, only legumain exhibited a significant fluorescent response, whereas the other species had negligible effects. A standard MTT assay was conducted to investigate the cytotoxicity of QM-AAN-CPP against normal cells (QSG-7701 cells). As shown in Figure S7, QM-AAN-CPP did not show obvious toxicity in QSG-7701 cells, thus this probe have low toxicity in the mouse model infected with schistosomes. All results indicated that the probe QM-AAN-CPP exhibited good stability and excellent selectivity toward legumain over other competitive analytes. Because the AAN substrate peptide served as a specific legumain-active trigger moiety, QM-AAN-CPP is a promising probe for tracking legumain in mouse models of schistosomiasis mansoni.

3.4. *Light-up tracking of endogenous legumain activity in Schistosomiasis mansoni*

After infection with schistosoma, cercaria progresses to adult worms in mammals (Fig. 3A). The diagnosis of schistosomiasis is routinely carried out using microscopy, which though affordable and highly specific, yet less sensitive. Especially when encountering cercaria, the detection effect is worse due to the small size (280–360 μm). Therefore, there is an urgent need to develop rapid and affordable diagnostics that are highly sensitive. Previous studies reported elevated legumain levels in *Schistosoma mansoni* worms [40]. Encouraged by the above *in vitro* results, we investigated whether QM-AAN-CPP could detect legumain activity in schistosomiasis mansoni. Hence, we tested the probe on schistosome cercaria and adult *Schistosoma mansoni* worms. As shown in Fig. 3B, after incubation with 25 μM QM-AAN-CPP for 2 h, schistosome cercaria exhibited weak AIE&NIR fluorescence, reflecting relatively low legumain activity. In contrast, both male (Fig. 3C) and female (Fig. 3D) adult *Schistosoma mansoni* worms exhibited robust red-channel AIE&NIR

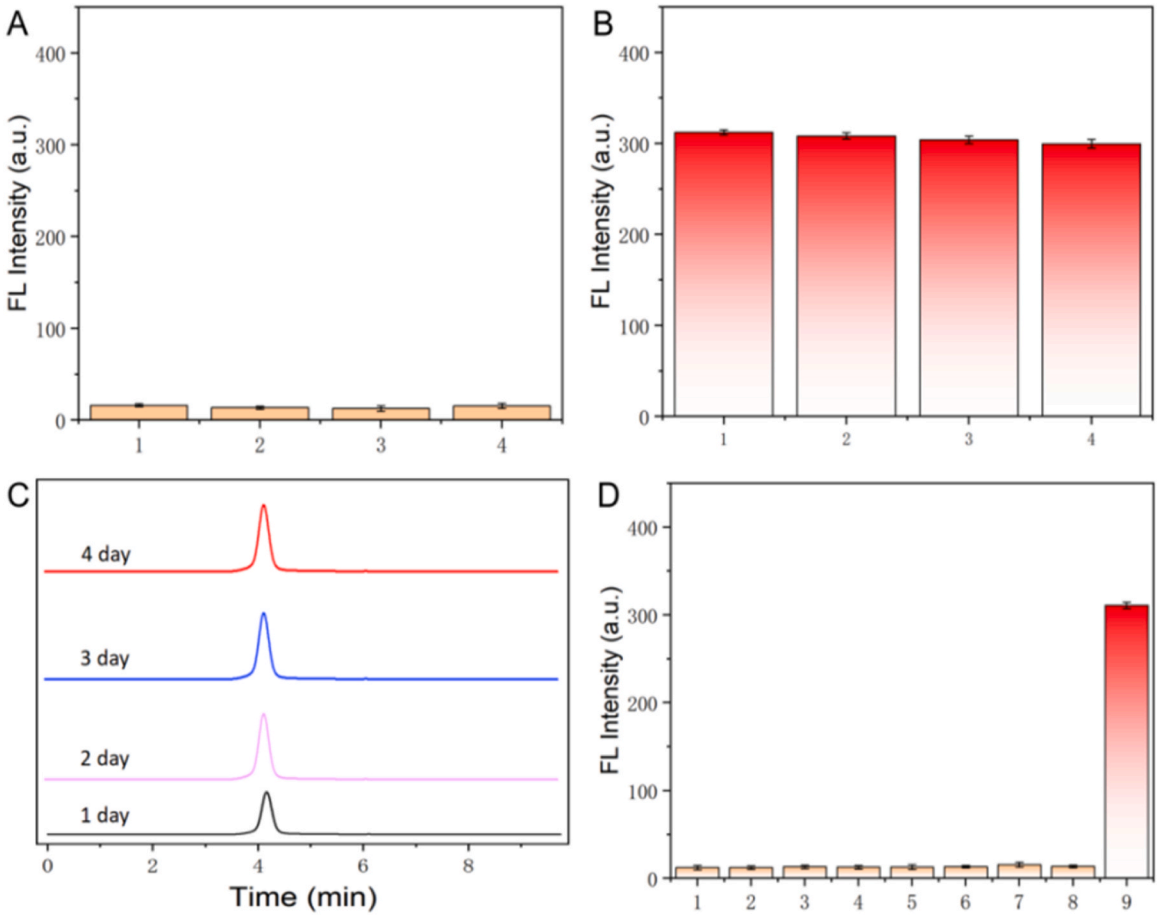

Fig. 2. Fluorescence intensity of QM-AAN-CPP (25 μM) incubated without (A) and with (B) legumain for up to 4 days. (C) HPLC traces of QM-AAN-CPP (25 μM) in 10 % FBS/medium at 37 °C monitored over 4 days. (D) Fluorescence responses of QM-AAN-CPP (25 μM) to various potential interferents: (1) blank, (2) GSH, (3) HCy, (4) Cys, (5) ClO^-, (6) H_2O_2, (7) LAP, (8) Cathepsin B, (9) Legumain. Data are shown as the mean ± standard deviation of three separate measurements. $\lambda_{ex} = 455$ nm.

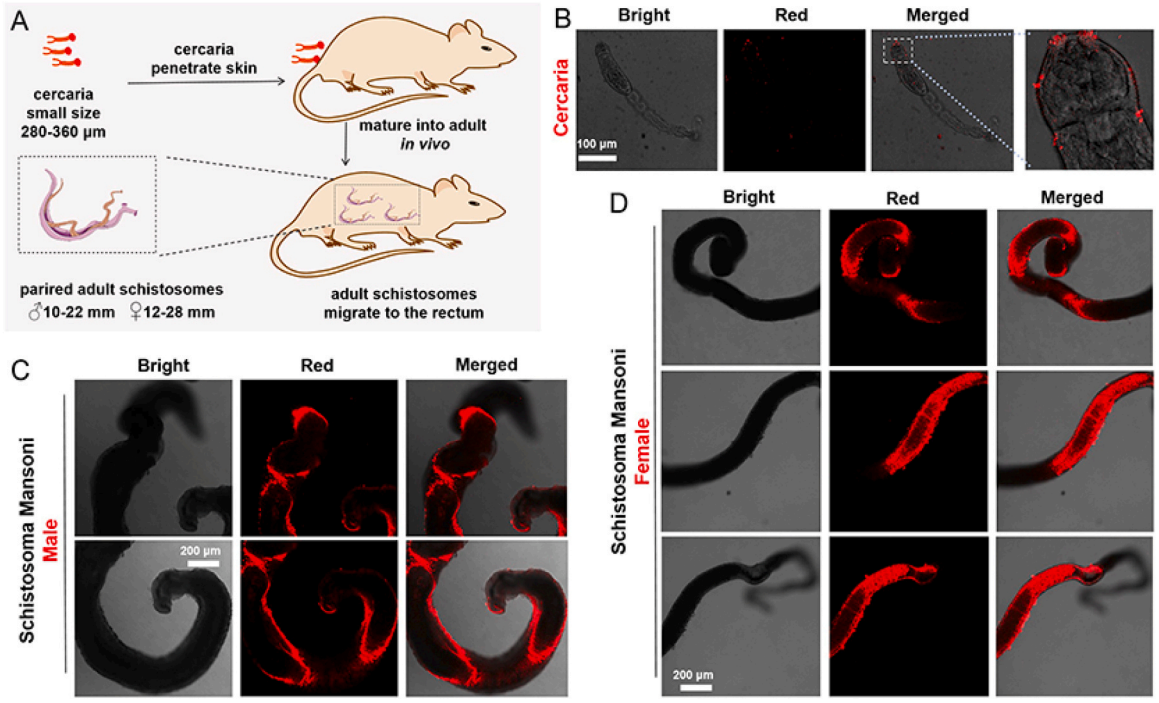

Fig. 3. (A) Showing the relationship between the schistosome cercaria and adult *Schistosoma mansoni* worms. Confocal laser scanning microscopy images of schistosome cercaria and adult *Schistosoma mansoni* worms, (B) Schistosome cercaria incubated with probe QM-AAN-CPP (25 μM) for 2 h. Male (C) and female (D) worms incubated with QM-AAN-CPP (25 μM) for 2 h. The red channel was collected from 600 to 700 nm, λ_{ex} = 455 nm.

fluorescence under the same conditions, with female adult worms displaying notably stronger fluorescence intensity than males. Additionally, bright-field images of *Schistosoma mansoni* showed an intact skin surface structure and overall good viability, indicating low toxicity at 25 μM QM-AAN-CPP. These results demonstrated that QM-AAN-CPP is well-suited for real-time fluorescence imaging of endogenous legumain in live *Schistosoma mansoni* showing an enhanced fluorescence signal.

To assess the utility of *in vivo* imaging of endogenous legumain activity in a schistosomiasis infection model, we administered QM-AAN-CPP (250 μM, 100 μL intravenous injection) to infected male mice and uninfected female mice. As shown in Fig. 4A, infected mice exhibited weak fluorescence on the epidermis after 2 h, likely because adult *Schistosoma mansoni* mainly reside in deeper intestinal regions behind internal organs. And the uninfected mice exhibited no fluorescence on the epidermis (Fig. 4B). Therefore, we dissected the mice to observe fluorescence signals in the intestinal areas. As shown in Fig. 4C, significant fluorescence signals were found in the intestinal regions of infected mice, whereas no fluorescence signal was observed in the intestinal regions of uninfected mice (Fig. 4D). Additionally, there was no fluorescent signal in other major organs, highlighting the high specificity of QM-AAN-CPP. Taken together, these findings confirm that this enzyme-activatable AIE probe QM-AAN-CPP is competent for *in vivo* real-time imaging of legumain activity and may facilitate rapid diagnosis of schistosomiasis mansoni. To quantitative analysis, the FL value for infected and uninfected was calculated (Fig. 4E). Obviously, the FL value of the probe in infected models is 20-fold than that of in uninfected models, indicating that the legumain levels are really high in Schistosoma mansoni.

4. Conclusions

In summary, we developed a schistosome-targeted AIE probe, QM-

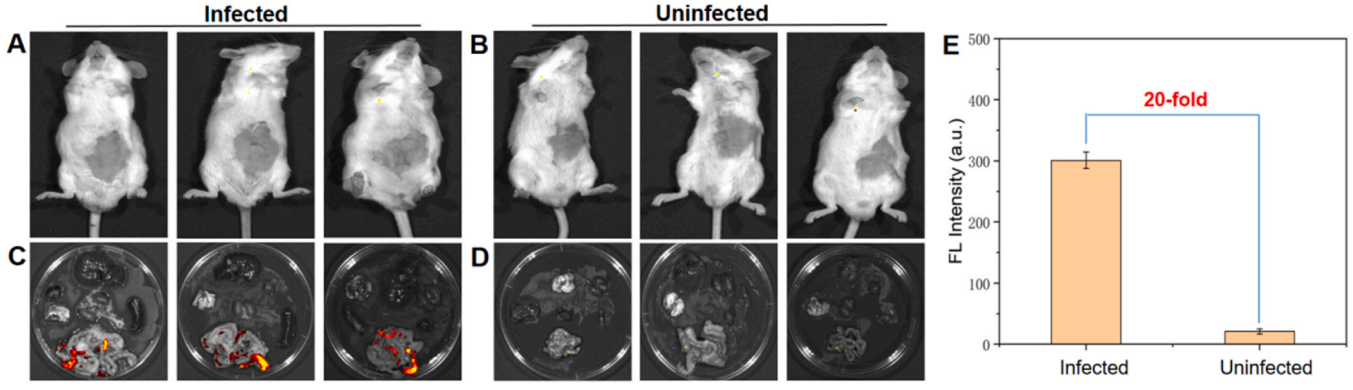

Fig. 4. Fluorescence imaging of legumain *in vivo* using a schistosomiasis infection model. Infected (A) and uninfected (B) mouse after intravenous injection of QM-AAN-CPP (250 μM, 100 μL). Ex vivo fluorescence images of major organs (heart, liver, spleen, lung, kidney, intestines) from the infected (C) and uninfected (D) mouse. (E) Comparison of fluorescence intensity of infected and uninfected mouse. Fluorescence emission was collected at 600–700 nm using the LECA spectrum imaging system with excitation at 455 nm.

AAN-CPP, for tracking legumain activity in schistosomiasis mansoni. This high-performance probe displays an AIE&NIR response to legumain with high sensitivity and selectivity, activated by specific endogenous enzymes. These characteristics, combined with excellent AIE photophysical properties and good cell membrane permeability, make QM-AAN-CPP highly suitable for tracing endogenous legumain activity. *In vivo* experiments using a living-body imager demonstrated that QM-AAN-CPP effectively distinguishes between infection with *Schistosoma mansoni* and uninfected controls. We believe that this enzyme-activatable AIE&NIR probe can serve as a powerful tool for elucidating the roles of endogenous legumain in *Schistosoma mansoni* and for facilitating the rapid diagnosis of schistosomiasis mansoni.

CRediT authorship contribution statement

Masceline Jenipher Mutsaka-Makuvaza: Formal analysis. **Zhiqiang Qin:** Formal analysis. **Qingchi Han:** Formal analysis. **Yingjun Qian:** Formal analysis. **Nicholas Midzi:** Formal analysis. **Chunli Cao:** Formal analysis, Data curation. **Liping Duan:** Formal analysis. **Yinlong Li:** Data curation. **Wangping Deng:** Data curation. **Zhiqian Guo:** Writing – review & editing, Conceptualization. **Qiang Li:** Writing – original draft, Formal analysis, Data curation, Conceptualization. **Xiaonong Zhou:** Formal analysis, Data curation. **Chenxu Yan:** Formal analysis, Data curation. **Shizhu Li:** Writing – review & editing, Data curation, Conceptualization. **Jing Xu:** Formal analysis.

Declaration of Competing Interest

The authors declare that they have no competing financial interests or personal relationships that could have appeared to influence the work reported in this paper.

Acknowledgments

This research was financially supported by the National Natural Science Foundation of China (No. 32161143036, No.32311540013, No.82473688), the National Key Research and Development Program of China (No. 2021YFC2300800, 2021YFC2300802), and Three-Year Initiative Plan for Strengthening Public Health System Construction in Shanghai (2023–2025) Key Discipline Project (No. GWVI-11.1–12).

Appendix A. Supporting information

Supplementary data associated with this article can be found in the online version at doi:10.1016/j.snb.2025.138626.

Data availability

Data will be made available on request.

References

[1] A.V. Díaz, M. Walker, J.P. Webster, Reaching the world health organization elimination targets for schistosomiasis: the importance of a one health perspective, Philos. Trans. R. Soc. B. 378 (2023) 20220274.
[2] O. Ally, B.N. Kanoi, L. Ochola, S.G. Nyanjom, C. Shiluli, G. Misinzo, J. Gitaka, Schistosomiasis diagnosis: challenges and opportunities for elimination, PLOS Negl. Trop. Dis. 18 (2024) e0012282.
[3] N.C. Lo, F.S.M. Bezerra, D.G. Colley, F.M. Fleming, M. Homeida, N. Kabatereine, F. M. Kabole, C.H. King, M.A. Mafe, N. Midzi, F. Mutapi, J.R. Mwanga, R.M.R. Ramzy, F. Satrija, J.R. Stothard, M.S. Traoré, J.P. Webster, J. Utzinger, X.N. Zhou, A. Danso-Appiah, P. Eusebi, E.S. Loker, C.O. Obonyo, R. Quansah, S. Liang, M. Vaillant, M.H. Murad, P.G. Hagan, Review of 2022 WHO guidelines on the control and elimination of schistosomiasis, Lancet Infect. Dis. 22 (2022) e327–e335.
[4] P.J. Hotez, D.H. Molyneux, A. Fenwick, J. Kumaresan, S.E. Sachs, J.D. Sachs, L. Savioli, Control of neglected tropical diseases, N. Engl. J. Med. 357 (2007) 1018–1027.
[5] P.H.L. Lamberton, C.L. Faust, J.P. Webster, Praziquantel decreases fecundity in schistosoma mansoni adult worms that survive treatment: evidence from a laboratory life-history trade-offs selection study, Infect. Dis. Poverty 6 (2017) 110.
[6] D.J. Berger, T. Crellen, P.H.L. Lamberton, F. Allan, A. Tracey, J.D. Noonan, N. B. Kabatereine, E.M. Tukahebwa, M. Adriko, N. Holroyd, J.P. Webster, M. Berriman, J.A. Cotton, Whole-genome sequencing of schistosoma mansoni reveals extensive diversity with limited selection despite mass drug administration, Nat. Commun. 12 (2021) 4776.
[7] J. Rivera, Y. Mu, C.A. Gordon, M.K. Jones, G. Cheng, P. Cai, Current and upcoming point-of-care diagnostics for schistosomiasis, Trends Parasitol. 40 (2024) 60–74.
[8] R.R.M. Lima, J.V.A. Lima, J.F.F. Ribeiro, J.B. Nascimento, W.F. Oliveira, P.E. C. Filho, A. Fontes, Emerging biomedical tools for biomarkers detection and diagnostics in schistosomiasis, Talanta 265 (2023) 124900.
[9] A. Kongs, G. Marks, P. Verlé, P.V. der Stuyft, The unreliability of the Kato-Katz technique limits its usefulness for evaluating S. Mansoni infections, Trop. Med. Int. Health 6 (2001) 163–169.
[10] C. Lv, W. Deng, L. Wang, Z. Qin, X. Zhou, J. Xu, Molecular techniques as alternatives of diagnostic tools in China as schistosomiasis moving towards elimination, Pathogens 11 (2022) 287.
[11] X. Wang, Q. Ding, R.R. Groleau, L. Wu, Y. Mao, F. Che, O. Kotova, E.M. Scanlan, S. E. Lewis, P. Li, B. Tang, T.D. James, T. Gunnlaugsson, Fluorescent probes for disease diagnosis, Chem. Rev. 124 (2024) 7106–7164.
[12] J. Ma, R. Sun, K. Xia, Q. Xia, Y. Liu, X. Zhang, Design and application of fluorescent probes to detect cellular physical microenvironments, Chem. Rev. 124 (2024) 1738–1861.
[13] H. Fang, Y. Chen, Z. Jiang, W. He, Z. Guo, Fluorescent probes for biological species and microenvironments: from rational design to bioimaging applications, Acc. Chem. Res. 56 (2023) 258–269.
[14] M.Q. Klinkert, R. Felleisen, G. Link, A. Ruppel, E. Beck, Primary structures of Sm31/32 diagnostic proteins of schistosoma mansoni and their identification as proteases, Mol. Biochem. Parasit. 33 (1989) 113–122.
[15] M. Poreba, Recent advances in the development of legumain selective chemical probes and peptide prodrugs, Biol. Chem. 400 (2019) 1529–1550.
[16] D. Jia, S. Chen, P. Bai, C. Luo, J. Liu, A. Sun, J. Ge, Cardiac resident macrophage-derived legumain improves cardiac repair by promoting clearance and degradation of apoptotic cardiomyocytes after myocardial infarction, Circulation 145 (2022) 1542–1556.
[17] P.J. Skelly, C.B. Shoemaker, Schistosoma mansoni proteases Sm31 (Cathepsin B) and Sm32 (Legumain) are expressed in the cecum and protonephridia of cercariae, J. Parasitol. 87 (2001) 1218–1221.
[18] A. Ruppel, U. Breternitz, R. Burger, Diagnostic M_r 31,000 schistosoma mansoni proteins: requirement of infection, but not immunization, and use of the "miniblot" technique for the production of monoclonal antibodies, J. Helminthol. 61 (1987) 95–101.
[19] A. Ruppel, H.J. Diesfeld, U. Rother, Immunoblot analysis of schistosoma mansoni antigens with sera of schistosomiasis patients: diagnostic potential of an adult schistosome polypeptide, Clin. Exp. Immunol. 62 (1985) 499–506.
[20] L.E. Edgington, M. Verdoes, A. Ortega, N.P. Withana, J. Lee, S. Syed, M. H. Bachmann, G. Blum, M. Bogyo, Functional imaging of legumain in cancer using a new quenched activitybased probe, J. Am. Chem. Soc. 135 (2013) 174–182.
[21] Y. Zhao, Z. Hai, H. Wang, L. Su, G. Liang, Legumainspecific near-infrared fluorescence "Turn On" for tumor-targeted imaging, Anal. Chem. 90 (2018) 8732–8735.
[22] F.Y. Zhu, L.J. Mei, R. Tian, C. Li, Y.L. Wang, S.L. Xiang, M.Q. Zhu, B.Z. Tang, Recent advances in super-resolution optical imaging based on aggregation-induced emission, Chem. Soc. Rev. 53 (2024) 3350–3383.
[23] M.H. Chua, K.L.O. Chin, X.J. Loh, Q. Zhu, J.W. Xu, Aggregation-induced emission-active nanostructures: beyond biomedical applications, ACS Nano 17 (2023) 1845–1878.
[24] W. Kang, M. Ma, S. Tang, Y. Wang, J. Li, L. Xu, P. Ma, D. Song, Y. Sun, A rapidly metabolizable and enzyme-activated NIR fluorescent probe based on isophorone for imaging *in vivo*, Sens. Actuators BChem. 419 (2024) 136299.
[25] R. Wang, X. Wang, X. Gu, Y. Liu, C. Zhao, Rationally designed fluorescent probes using target specific cascade reactions, Sens. Actuators BChem. 380 (2023) 133282.
[26] Z. Guo, C. Yan, W.-H. Zhu, High-performance quinoline-malononitrile core as a building block for the diversity-oriented synthesis of AIEgens, Angew. Chem. Int. Ed. 59 (2020) 9812–9825.
[27] Q. Liu, C. Sun, R. Dai, C. Yan, Y. Zhang, W.-H. Zhu, Z. Guo, Engineering *h*igh-performance dicyanomethylene-4H-pyran fluorophores for biosensing and phototherapy, Coord. Chem. Rev. 503 (2024) 215652.
[28] M. Wang, M. Tao, W. Zhu, W. Liu, Z. Liu, Z. Hai, Tumor-targeted fluorescent/photoacoustic imaging of legumain activity *in vivo*, ACS Sens. 8 (2023) 4473–4477.
[29] C. Lu, K. Li, H. Xi, D. Hua, H. Li, F. Gao, L. Qiu, J. Lin, Dual-targeting PET tracers enable enzyme-mediated self-assembly for the PET imaging of legumain activity, ACS Appl. Mater. Interfaces 15 (2023) 44654–44664.
[30] A. Saha, S. Mandal, J.V.V. Arafiles, J. Gómez-González, C.P.R. Hackenberger, A. Brik, Structure-uptake relationship study of DABCYL derivatives linked to cyclic cell-penetrating peptides for live-cell delivery of synthetic proteins, Angew. Chem. Int. Ed. 61 (2022) e202207551.
[31] A. Gori, G. Lodigiani, S.G. Colombarolli, G. Bergamaschi, A. Vitali, Cell penetrating peptides: classification, mechanisms, methods of study, and applications, ChemMedChem 18 (2023) e202300236.
[32] Y. Wu, G. Zeng, N. Lvyue, W. Wu, T. Jiang, R. Wu, W. Guo, X. Li, X. Fan, Triethylene glycol-modified iridium (iii) complexes for fluorescence imaging of schistosoma japonicum, J. Mater. Chem. B 5 (2017) 4973–4980.

[33] J.A. Clegg, S.R. Smithers, The effects of immune rhesus monkey serum on schistosomula of schistosoma mansoni during cultivation *in vitro*, Int. J. Parasitol. 2 (1972) 79–98.
[34] Y. Lyu, X. Chen, Q. Wang, Q. Li, Q. Wang, X. Li, Z. Zhu, C. Yan, X. Zhao, W.-H. Zhu, Monitoring autophagy with Atg4B protease-activated aggregation-induced emission probe, Adv. Funct. Mater. 32 (2022) 2108571.
[35] J. Li, M. Zhao, J. Huang, P. Liu, X. Luo, Y. Zhang, C. Yan, W.-H. Zhu, Z. Guo, A "crossbreeding" dyad strategy for bright and small-molecular weight near-infrared fluorogens: from the structural design to boost aggregation-induced emission, Coord. Chem. Rev. 473 (2022) 214813.
[36] J. Ge, W. Cai, N. Niu, Y. Wen, Q. Wu, L. Wang, D. Wang, B.Z. Tang, R. Zhang, Viscosity-responsive NIR-II fluorescent probe with aggregation-induced emission features for early diagnosis of liver injury, Biomaterials 300 (2023) 122190.
[37] J. Mulvenna, L. Moertel, M.K. Jones, S. Nawaratna, E.M. Lovas, G.N. Gobert, M. Colgrave, A. Jones, A. Loukas, D.P. McManus, Exposed proteins of the schistosoma japonicum tegument, Int. J. Parasitol. 40 (2010) 543–554.
[38] C.R. Caffrey, J.H. McKerrow, J.P. Salter, M. Sajid, Blood 'n'guts: an update on schistosome digestive peptidases, Trends Parasitol. 20 (2004) 241–248.
[39] E. Dall, H. Brandstetter, Structure and function of legumain in health and disease, Biochimie 122 (2016) 126–150.
[40] M. Poreba, Recent advances in the development of legumainselective chemical probes and peptide prodrugs, Biol. Chem. 400 (2019) 1529–1550.